AIP Applied Physics Letters

Undoped vacuum annealed In 2 O 3 thin films as a transparent conducting oxide

A. Dixit, C. Sudakar, R. Naik, V. M. Naik, and G. Lawes

Citation: Applied Physics Letters **95**, 192105 (2009); doi: 10.1063/1.3262963
View online: http://dx.doi.org/10.1063/1.3262963
View Table of Contents: http://scitation.aip.org/content/aip/journal/apl/95/19?ver=pdfcov
Published by the AIP Publishing

Articles you may be interested in
Radio-frequency superimposed direct current magnetron sputtered Ga:ZnO transparent conducting thin films
J. Appl. Phys. **111**, 093718 (2012); 10.1063/1.4709753

Electrical and optical properties of transparent conducting In4+xSn3−2xSbxO12 thin films
J. Appl. Phys. **110**, 033702 (2011); 10.1063/1.3605552

High near-infrared transparency and carrier mobility of Mo doped In 2 O 3 thin films for optoelectronics applications
J. Appl. Phys. **106**, 063716 (2009); 10.1063/1.3224946

Improved near-infrared transparency in sputtered In 2 O 3 -based transparent conductive oxide thin films by Zr-doping
J. Appl. Phys. **101**, 063705 (2007); 10.1063/1.2711768

Properties of transparent conductive In 2 O 3 :Mo thin films deposited by Channel Spark Ablation
J. Vac. Sci. Technol. A **23**, 1350 (2005); 10.1116/1.1991871

This article is copyrighted as indicated in the article. Reuse of AIP content is subject to the terms at: http://scitation.aip.org/termsconditions. Downloaded to IP: 128.123.44.23 On: Mon, 22 Dec 2014 22:59:35

Undoped vacuum annealed In_2O_3 thin films as a transparent conducting oxide

A. Dixit,[1] C. Sudakar,[1] R. Naik,[1] V. M. Naik,[2] and G. Lawes[1,a)]
[1]*Department of Physics and Astronomy, Wayne State University, Detroit, Michigan 48201, USA*
[2]*Department of Natural Sciences, University of Michigan–Dearborn, Dearborn, Michigan 48128, USA*

(Received 22 September 2009; accepted 21 October 2009; published online 10 November 2009)

We have investigated the structural, optical, and electrical properties of both as-grown and vacuum annealed In_2O_3 thin films. In contrast to the insulating as-prepared samples, vacuum annealed In_2O_3 films exhibit a metallic electrical conductivity with increased carrier concentration and mobility. We attribute the excess carriers to an oxygen deficiency introduced during vacuum annealing. Remarkably, these carrier densities seem to be stable under ambient conditions for at least two years. Optical spectroscopy measurements show a large optical transparency, greater than 80%, for both the as-prepared and vacuum annealed In_2O_3 films. © *2009 American Institute of Physics*.
[doi:10.1063/1.3262963]

Transparent conducting oxides (TCO) combine the properties of high optical transparency at visible wavelengths with high electrical conductivity. These materials are important for many optoelectronic applications including photovoltaic and photoelectrochemical devices, liquid crystal displays and light emitting diodes.[1] These materials should have a wide bandgap, above roughly 3 eV to avoid optical excitations in the visible wavelengths, but also a high electrical conductivity. The coexistence of these two contraindicated material properties has been identified in a number of metal oxides including ZnO,[2] CdO,[3] SnO_2,[4] and In_2O_3.[3] A high electrical conductivity in these metal oxides is usually produced by doping higher valence cations, which act as donor source for excess electrons, resulting in n-type conduction. Among the most common n-type TCOs used for solar cells and various optoelectronic applications are Al doped ZnO,[5] F doped SnO_2,[6] and Sn doped In_2O_3.[7]

Among various metal oxides, indium oxide based TCOs typically show the lowest resistivity.[8] There remains some debate on the value of bandgap of In_2O_3. Early studies found a direct optical bandgap of ~ 3.75 eV with an onset of indirect phonon assisted transitions starting at ~ 2.6 eV. More recent theoretical[9] and x-ray photoelectron spectroscopy studies show that band-edge transitions in In_2O_3 are forbidden because of the even parity for states at both the top of valence band and the bottom of conduction band, which prohibits dipole transitions. These studies also proposed a strong optical transition from 0.8 eV below the top of the valence band to the conduction band. These theoretical studies coupled with recent optical measurements on high quality epitaxial indium oxide thin films[10] suggest a lower intrinsic direct bandgap value ~ 2.6 eV in contrast to previously accepted value ~ 3.75 eV.

This proposed small bandgap for indium oxide may play a critical role in establishing the performance of In_2O_3 as a TCO. It has been argued that surface charges pin the Fermi level of In_2O_3 0.4 eV above the minimum of the conduction band, which accounts for the coexisting large carrier concentration with large optical bandgap and may also explain the tendency for In_2O_3 to express n-type conductivity.[11] It is also suggested that doped In_2O_3 can support a high carrier density without forming compensating acceptor defects, even for large dopant concentrations.[12] This may explain why In_2O_3 has more stable, higher electrical conductivity than other undoped/doped oxides. Previous studies on Sn doped and undoped In_2O_3 annealed under a variety of conditions show that this system can often develop significant electrical conductivity while remaining optically transparent.[13] In contrast, conducting ZnO thin films do not exhibit long term electrical stability because of the chemisorption of oxygen at grain boundaries.[14,15] This oxygen forms localized extrinsic trap states at grain boundaries, trapping free electrons and creating local potential barriers, which result in a reduced conductivity and mobility. It has also been suggested recently that hydrogen may form shallow donor centers in In_2O_3, which can dramatically affect the conductivity in this system.[16]

To investigate indium oxide as a transparent conducting oxide, we deposited In_2O_3 thin films on c-axis (0001) sapphire substrates by radio frequency (13.56 MHz) magnetron sputtering using a high purity (5 N) In metal target. These films were grown at $T=475\pm 5$ °C with a forward rf power of 100 W. The total working pressure in the chamber was held at 1.5×10^{-2} Torr with an optimized ratio of high purity oxygen and argon as reactive and sputtering gases. The thickness of the films used in this study was ~ 1 μm. A cross sectional scanning electron micrograph of an as-grown (AG) In_2O_3 film is shown in Fig. 1(a). To explore the possibility of using these films as a TCO material, we annealed the films under high vacuum with a base pressure less than 10^{-6} Torr, at a temperature of 600 °C for 9 h to introduce oxygen vacancies. While shorter annealing times and different temperatures also resulted in an increase in conductivity, these conditions yielded the best electrical transport properties.

We plot x-ray diffraction (XRD) patterns for the AG and vacuum annealed (VA) samples in Figs. 1(b) and 1(c). The diffraction peaks could be completely indexed to the cubic bixbyite In_2O_3 structure, consistent with a polycrystalline film. The intense peaks at $2\theta=30.86°$ and 63.86° in Figs. 1(b) and 1(c) correspond to the (222) and (444) reflections, suggesting the films are highly textured along the (222) orientation. However, the insets in Figs. 1(b) and 1(c), which plot the data on a semilog plot, shows the additional In_2O_3

a)Electronic mail: glawes@wayne.edu.

 © 2009 American Institute of Physics

This article is copyrighted as indicated in the article. Reuse of AIP content is subject to the terms at: http://scitation.aip.org/termsconditions. Downloaded to IP: 128.123.44.23 On: Mon, 22 Dec 2014 22:59:35

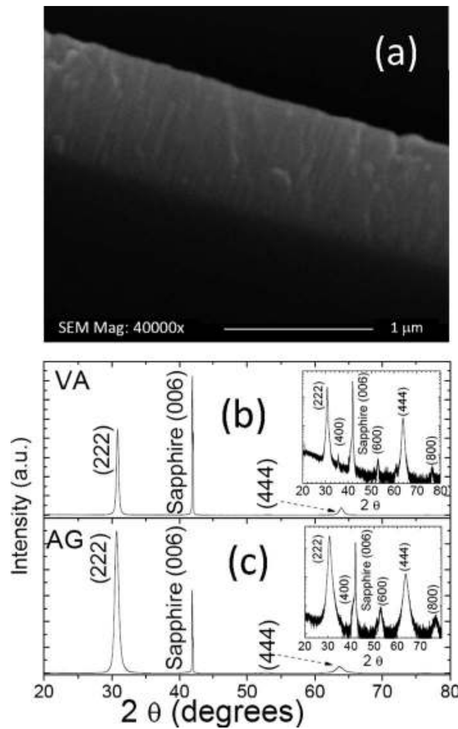

FIG. 1. (a) Cross-sectional SEM of an as-deposited In_2O_3 film. (b) XRD for a vacuum annealed In_2O_3 thin film and (c) XRD for an as-prepared In_2O_3 thin film.

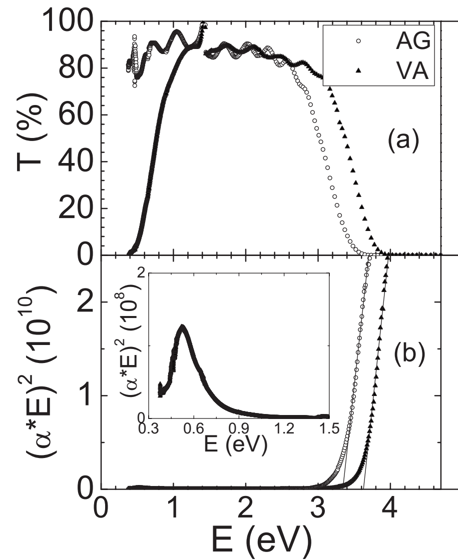

FIG. 2. (a) Optical transmission spectra for as grown (open circles) and vacuum annealed (VA: closed triangles) In_2O_3 thin films. (b) Optical absorption coefficient plotted as $(\alpha\cdot E)^2$. The straight lines show the linear regression fit over the values described in the text. Inset: Optical absorption spectrum plotted on a reduced scale to show the plasmon peak near 0.5 eV in VA sample.

reflections, demonstrating the polycrystalline nature of the samples. The lattice parameter for both the AG and VA thin films is 10.069 Å, showing that the crystal structure is unaffected by vacuum annealing despite the oxygen deficiency. The Bragg peaks for the VA sample are likely to become sharper than those for the AG sample because the vacuum annealing is done at a higher temperature, which is likely to improve the crystallinity of the sample. We find no evidence for the formation of any secondary phase on vacuum annealing. The cross-sectional image in Fig. 1(a) shows the (222) oriented columnar grains of In_2O_3.

We used optical spectroscopy to investigate the optical properties of these AG and VA In_2O_3 films. We measured the optical transmittance and reflectance spectra from 175 to 3300 nm; the results of these transmission measurements are plotted in Fig. 2(a). Both films are transparent, having transmittance values of approximately 85% or higher. The spectrum for the vacuum annealed In_2O_3 thin film show a sharp decrease in the low energy transmittance, indicating the onset of plasmon absorption at ~0.5 eV. We calculated the absorption coefficient from these transmittance and reflectance data and plot the result in the form of $(\alpha\cdot E)^2$ versus E in Fig. 2(b). We determined the optical absorption edge by extrapolating $(\alpha\cdot E)^2$, considering the linear region $3\times10^9 < (\alpha\cdot E)^2 < 2\times10^8$, to E=0. The optical bandgaps for the AG and VA samples are found to be 3.3 ± 0.1 eV and 3.6 ± 0.1 eV, with the uncertainty arising from the fact that different fitting ranges leading to slightly different bandgap values. We show the low energy absorption coefficient on a reduced scale in the inset to Fig. 2(b). On this scale, the plasmon peak can be clearly discerned near 0.5 eV.

The relative increase in the optical bandgap on vacuum annealing can be attributed to the filling of the conduction band with additional n-type carriers, producing a Burstein–Moss shift.[17,18] The Burstein–Moss shift ΔE_{BM} using the free electron approximation is given as $\Delta E_{MB} = h^2/8\pi^2 m^*(3\pi^2 n_e)^{2/3}$, where m^* is the electron effective mass, h is the Planck constant, and n_e is the electron carrier concentration. Assuming $\Delta E_{BM}=0.3$ eV and $m^*=0.3\ m_e$ for In_2O_3,[19] where m_e is electron mass, the estimated carrier concentration is computed to be $n_e \sim 2.1\pm0.4\times10^{20}$ cm^{-3}, considering only the error derived from the uncertainty in ΔE_{BM}. This value is in good agreement with the carrier density calculated using the plasmon frequency, discussed below, and room temperature Hall measurements on the VA samples.

We applied the Drude model to analyze the optical response of the vacuum annealed In_2O_3 thin films and fit the reflectance data using the plasmon frequency and damping constant as fitting variables. We determined that the plasmon peak fell at ~0.48 eV, consistent with the energy extracted from transmittance/reflectance measurements. Using this value, we determined the carrier density from the value of the high frequency dielectric constant ($\varepsilon_\infty=3.964$) (Ref. 20) and electron effective mass ($0.3m_e$) (Ref. 19) appropriate for In_2O_3. The carrier density extracted for the VA thin film is 2.1×10^{20} cm^{-3}, which is consistent with the value estimated from the Burstein–Moss shift. The calculated mobilities, extracted from Hall effect measurements, for AG and VA thin films were 1 and 40 cm^2/V·s.

We measured the temperature dependent resistivity of the AG and vacuum annealed In_2O_3 thin film samples from 10 to 350 K, as shown in Fig. 3. The AG In_2O_3 thin film show semiconductor behavior, whereas the vacuum annealed thin film shows metallic resistivity, having a much smaller value compared to that of the AG sample. On vacuum annealing, the carrier concentration increases by two orders of magnitude and the Hall mobility increases sharply, both of which combine to produce a large drop in resistivity. The resistivity of the vacuum annealed In_2O_3 film remains metallic, but almost constant, over almost the entire temperature range, having a very shallow resistivity minimum near 80 K.

This article is copyrighted as indicated in the article. Reuse of AIP content is subject to the terms at: http://scitation.aip.org/termsconditions. Downloaded to IP: 128.123.44.23 On: Mon, 22 Dec 2014 22:59:35

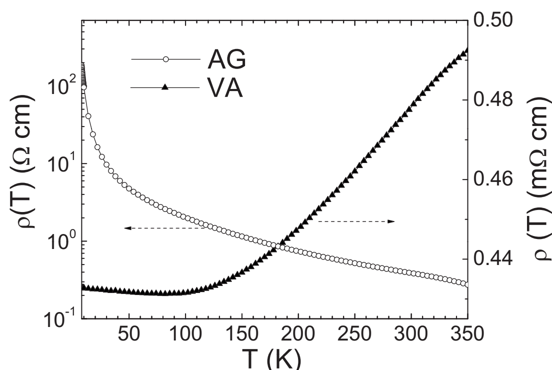

FIG. 3. Resistivity of as grown (AG: open circles) and vacuum annealed (VA: closed triangles) In_2O_3 thin films. Note that the resistivity for the AG film is plotted using a logarithmic scale and the y-axes have different units.

The figure of merit for conducting oxides, $F_H = T^{10}/R_s$, where T is the optical transmittance at a specific wavelength ($\lambda = 550$ nm) and R_s is the sheet resistance in units of $\Omega/\square$,[21] for VA In_2O_3 thin films is $\sim 1.2 \times 10^{-2}\ \Omega/\square$. This value is somewhat lower but still comparable to that of commercial ITO thin films $\sim 5.9 \times 10^{-2}\ \Omega/\square$.[22]

As oxygen deficient films often oxidize rapidly in ambient conditions, we also tested the long-term stability of these samples. We measured the resistivity of over a half-dozen VA In_2O_3 thin films that were stored under ambient conditions for periods from six months to two years after vacuum annealing. For all samples, the room temperature resistivity was found to fall in the range of 5×10^{-4} to $5 \times 10^{-3}\ \Omega$ cm, with no systematic dependence of resistivity on time after annealing. In all cases, this is two to three orders of magnitude smaller than the resistivity of the as-grown films but consistent with the resistivity measured immediately after vacuum annealing. We ascribe the non-negligible sample-to-sample variation in the resistivity of these VA films to unexpected differences in the specific annealing conditions. We believe that the resistivity is very sensitive to the precise oxygen stoichiometry, so fluctuations in the vacuum annealing conditions that affect the oxygen content can have a significant effect on the electrical properties of the In_2O_3 films.

In summary, we show that vacuum annealed In_2O_3 thin films exhibit high electrical conductivity and large optical bandgap ~3.6 eV. The observed carrier concentration and Hall mobility values are $\sim 10^{20}$ cm^{-3} and 40 cm^2/V·s. These vacuum annealed In_2O_3 thin films are stable over a length of time. The excess carriers, likely generated due to an oxygen deficiency in the vacuum annealed films, fill the conduction band, resulting in an increased optical bandgap. The stable increased optical bandgap together with high electrical conductivity make the vacuum annealed In_2O_3 thin films useful as conducting transparent oxide material without the need of any dopant.

This work has been supported by the NSF through Grant No. DMR-06044823.

[1]H. L. Hartnagel, A. L. Dawar, A. K. Jain, and C. Jagadish, *Semiconducting Transparent Thin Films* (Institute of Physics, Bristol, 1995); J. F. Wager, D. A. Keszler, and R. E. Presley, *Transparent Electronics* (Springer, New York, 2008).
[2]P. H. Jefferson, S. A. Hatfield, T. D. Veal, P. D. C. King, C. F. McConville, J. Auniga-Perez, and V. Munoz-Sanjose, Appl. Phys. Lett. **92**, 022101 (2008).
[3]I. Hamberg, C. G. Granqvist, K. F. Berggren, B. E. Sernelius, and L. Engstrom, Phys. Rev. B **30**, 3240 (1984).
[4]J. Robertson, Phys. Rev. B **30**, 3520 (1984); R. G. Egdell, J. Rebane, T. J. Walker, and D. S. L. Law, *ibid.* **59**, 1792 (1999).
[5]H. Kim, J. S. Horwitz, S. B. Qadri, and D. B. Chrisey, Thin Solid Films **420**, 107 (2002); K. Ellmer, A. Klein, and B. Rech, *Transparent Conductive Zinc Oxide* (Springer, New York, 2008).
[6]R. Riveros, E. Romero, and G. Gordillo, Braz. J. Phys. **36**, 1042 (2006); T. Minami, H. M. Sato, H. Nanto, and S. Takata, Jpn. J. Appl. Phys., Part 2 **25**, L776 (1986); J. W. Bae, S. W. Lee, and G. Y. Yeom, J. Electrochem. Soc. **154**, D34 (2007).
[7]H. Ohta, M. Orita, M. Hirano, H. Tanji, H. Kawazoe, and H. Hosono, Appl. Phys. Lett. **76**, 2740 (2000).
[8]G. J. Exarhos and X. D. Zhou, Thin Solid Films **515**, 7025 (2007).
[9]A. Walsh, J. L. F. Da Silva, S. H. Wei, C. Korber, A. Klein, L. F. J. Piper, A. DeMasi, K. E. Smith, G. Panaccione, P. Torelli, D. J. Payne, A. Bourlange, and R. G. Egdell, Phys. Rev. Lett. **100**, 167402 (2008).
[10]A. Bourlange, D. J. Payne, R. G. Egdell, J. S. Foord, P. P. Edwards, M. O. Jones, A. Schertel, P. J. Dobson, and J. L. Hutchison, Appl. Phys. Lett. **92**, 092117 (2008).
[11]P. D. C. King, T. D. Veal, D. J. Payne, A. Bourlange, R. G. Egdell, and C. F. McConville, Phys. Rev. Lett. **101**, 116808 (2008).
[12]S. B. Zhang, S. H. Wei, and A. Zunger, Phys. Rev. Lett. **84**, 1232 (2000).
[13]Y. Zhou and P. J. Kelly, Thin Solid Films **469**, 18 (2004).
[14]A. P. Roth and D. F. Williams, J. Appl. Phys. **52**, 6685 (1981).
[15]S. Major, A. Banerjee, and K. L. Chopra, Thin Solid Films **143**, 19 (1986).
[16]P. D. C. King, R. L. Lichti, Y. G. Celebi, J. M. Gil, R. C. Vilao, H. V. Alberto, J. Piroto Duarte, D. J. Payne, R. G. Egdell, I. McKenzie, C. F. McConville, S. F. J. Cox, and T. D. Veal, Phys. Rev. B **80**, 081201 (2009).
[17]E. Burstein, Phys. Rev. **93**, 632 (1954).
[18]T. S. Moss, Proc. Phys. Soc. London, Sect. B **67**, 775 (1954).
[19]F. Fuchs and F. Bechstedt, Phys. Rev. B **77**, 155107 (2008).
[20]C. H. L. Weijtens and P. A. C. van Loon, Thin Solid Films **196**, 1 (1991); Y. Ohhata, F. Shinoki, and S. Yoshida, *ibid.* **59**, 255 (1979).
[21]G. Haacke, J. Appl. Phys. **47**, 4086 (1976).
[22]M. Nisha, S. Anusha, A. Antony, R. Manoj, and M. K. Jayaraj, Appl. Surf. Sci. **252**, 1430 (2005).

This article is copyrighted as indicated in the article. Reuse of AIP content is subject to the terms at: http://scitation.aip.org/termsconditions. Downloaded to IP: 128.123.44.23 On: Mon, 22 Dec 2014 22:59:35